R. & M. No. 3440

MINISTRY OF AVIATION

AERONAUTICAL RESEARCH COUNCIL
REPORTS AND MEMORANDA

Design of a Supersonic Nozzle

By A. McCabe, Ph.D.

LONDON: HER MAJESTY'S STATIONERY OFFICE
1967
PRICE 15*s.* 6*d.* NET

Design of a Supersonic Nozzle

By A. McCabe, Ph.D.

The Mechanics of Fluids Department, University of Manchester

Communicated by Prof. N. H. Johannesen

Reports and Memoranda No. 3440*
March, 1964

Summary.—This paper presents a method of design of a supersonic nozzle which incorporates recent developments in compressible flow theory. Continuous curvature of the contour is ensured by defining a continuous gradient of Prandtl-Meyer angle along the nozzle axis. The flow in the throat was calculated from results given by Hall (1962). A matching technique was used to determine a triplet of values for the throat radius of curvature, the flow deflection at the inflection point and the Prandtl-Meyer angle at the point on the nozzle axis where the left-running characteristic through the inflection point intersects the nozzle axis.

The majority of the new work is to be found in the Appendices. Appendix B presents a method of determining the co-ordinates along a particular characteristic by inverting the results given by Hall[1] (1962). Appendix C reviews the accuracy of the method of characteristics and, Appendix D suggests a method by which it may be possible to increase the accuracy without resorting to calculations made at very small step sizes.

CONTENTS

*Replaces A.R.C. 25 716.

LIST OF CONTENTS—*continued*

1. *Introduction.*

1.1. *General Introduction.*

Although the literature on the design of supersonic nozzles is extensive there are very few tabulated ordinates available for working section Mach numbers greater than 2·0. Many of the ordinates which are available are based on design methods which are to some extent unsatisfactory. The errors introduced are indeed small but they are certainly not negligible in comparison with the manufacturing tolerances which are imposed. In view of the advanced state of knowledge in the field of compressible flow, it should now be possible to design the inviscid core of a supersonic nozzle quickly and sufficiently accurately to make the design errors small compared with the manufacturing errors. It may be argued that such accuracy is not required in view of the uncertainty introduced by adding a calculated boundary layer allowance, but this does not seem sufficient reason for introducing a further uncertainty by using an inaccurate method to design the inviscid core.

A nozzle to produce a uniform stream of Mach number 3·0 was required and it was decided to design the inviscid core sufficiently accurately for the ordinates to be correct to $\pm 0{\cdot}0002$ inches. The half height of the nozzle at the test section was to be about 2·5 inches, so that the half height at the throat was approximately 0·6 inches.

In supersonic nozzle design the conventional two-dimensional nozzle is usually considered to consist of several regions as shown in Fig. 1. These are:—

(i) the contraction, in which the flow is entirely subsonic,

(ii) the throat region, in which the flow accelerates from a high subsonic to a low supersonic speed,

(iii) an initial expansion region, where the slope of the contour increases up to its maximum value,

(iv) the straightening or 'Busemann' region in which the cross sectional area increases but the wall slope decreases to zero, and

(v) the test section, where the flow is uniform and parallel to the axis.

A good approximation to the throat height can be obtained by one-dimensional flow considerations. The error is small, being of the order of R^{-2} where R is the ratio of the radius of curvature of the nozzle wall at the throat to the throat half height; it is only 0·1 per cent when $R = 5{\cdot}2$.

From practical considerations the length of the nozzle should not be too great. There is, however, a minimum length below which it is not possible to design a nozzle which will accelerate the flow smoothly. This minimum length is usually regarded as the length of the nozzle which has a sharp-edged throat, the flow being turned from a parallel sonic stream through a centred expansion wave. Some doubts have been raised (Lord[2] (1961)) about this being the absolute minimum and the question is discussed more fully in Section 1.2. Tables of co-ordinates of the sharp-cornered nozzles are given by Edelman[3] (1948) and Shames and Seashore[4] (1948). However, this type of nozzle is impractical owing to viscous effects in the region close to the corner, and experience has shown that it is advisable to exceed the 'minimum' length by about 30 per cent.

In 1931, Busemann[5] gave a construction for a nozzle to convert divergent radial supersonic flow in two dimensions into a uniform supersonic stream of higher Mach number. This method was graphical and approximate so that it was subject to protractor errors, and afforded no means of determining the length of the nozzle in advance. The maximum expansion angle which will produce a desired flow in the test section without requiring compression waves is one half the Prandtl-Meyer angle of the desired flow. Puckett[6] (1946) pointed out that smaller expansion angles than the maximum were possible. The resulting nozzle would be longer but might have a more uniform final flow. Puckett also suggested the possibility of assuming a uniform radial flow at the maximum slope cross-section. Only the flow region downstream of the inflection point need then be calculated, and a smooth curve could be faired back to the throat from the inflection point.

Using this type of approach an analytic expression for the contour downstream of the radial flow region was found by Atkin[7] (1945) and by Foelsch[8] (1946). Atkin converted a uniform parallel low supersonic stream into a divergent radial flow. This radial flow was then converted into a uniform parallel supersonic flow at the desired Mach number by a 'Busemann' or straightening contour. The design was completed by adding a suitable initial contour. A similar derivation of these analytical relations was given by Foelsch. Foelsch also provided a means of designing a suitable contour to convert uniform radial supersonic flow into uniform parallel supersonic flow. This approach was adopted by Beckwith and Moore[9] (1955); they also started with a straight sonic line at the throat, normal to the axis of symmetry of the nozzle, and improved the method by computing the contour between the throat and the inflection point using the method of characteristics.

A nozzle design which does not directly employ the mathematical method of characteristics was evolved by Friedrichs[10] (1944). A series solution of the non-linear wave equation was used, only the leading terms in the series being retained in the design proper. This method was expanded by Nilson[11] (1948) and used by Baron[12] (1954) as a basis for the design of a number of nozzles.

Practical requirements concerning nozzle handling and time delays during test periods have brought forth methods which permit a quick change from one Mach number to another. One of the developments has been the production of variable-Mach-number nozzles jack-supported flexible steel sheets. However, an incompatibility between the aerodynamic and structural requirements is introduced if a point of discontinuous curvature exists at the inflection point. This has led to the development of continuous-curvature nozzles which are necessarily of longer length, e.g. see Riise[13] (1954), Rosen[14] (1955) and Sivells[15] (1955). Even with solid nozzles it is convenient to have continuous curvature of the walls. By this means the rate of growth of the boundary layer is kept continuous which makes it easier to correct the inviscid contour for boundary-layer growth and, therefore, helps to produce a more uniform flow in test section.

In the present design it was decided to follow Foelsch[8], Beckwith and Moore[9] and others in prescribing part of the supersonic flow field to be a region of radial flow. It was considered an advantage, however, to prescribe this region to lie within the nozzle in order to avoid straight segments in the contour which might lead to discontinuities in the rate of boundary-layer growth on the walls. The radial-flow region is shown as region IIIb in Fig. 2, touching the contour at the point of inflection. The present design may be considered to be a modification of Beckwith and Moore's method, account being taken of the more recent

advances for the calculation of the flow in the throat region. At the same time the opportunity has been taken to include a matching region IVa, which by maintaining continuity of the axial velocity gradient ensures continuity of the nozzle curvature at point K, a desirable feature missing in many nozzle design methods.

The other matching region IIIa was computed by the method of characteristics starting from known conditions along HB, BP and PI. To keep BP short and to maintain continuity of wall curvature it is desirable that both Mach number M and Mach number gradient be continuous at points B and P. The Mach number gradient in the radial flow region is a function of Mach number only, whereas the Mach number gradient at B is strongly dependent upon R. The gradients in both cases are shown in Fig. 3 for various values of r^* and R respectively, where r^* represents the distance between the virtual origin of the radial flow and the sonic circle. Since the analytic theory used in the throat region is only valid over a small section it is clear that perfect matching, i.e. with B and P coincident, is not possible unless the design Mach number is close to unity, and thus, a compromise is usually required. In the present case R was chosen to be equal to 5, θ_I to be 16·70° ($r^* = 3{\cdot}42785$) and a parabolic distribution of M was assumed between B and P. In general, it would be more convenient to work in terms of ν rather than M since ν is used in the characteristic calculations. For this reason the equations in the next section are given in terms of ν.

1.2. *The Question of Minimum Length.*

The axial distribution of ν between points B and P must be chosen in such a way that limit lines do not occur in the flow field inside the nozzle. Some consideration of the question has been given by Lord[2] (1961) but precise criteria are not available and it appears to be questionable whether or not precise criteria can be given. A reasonable, although indirect, criterion is to ensure that the intersection of the branch line* with the characteristic DJ (Fig. 2) lies on or outside the nozzle contour. This criterion appears to have been suggested by Friedrichs[10] (1944)† but as his paper is not readily available the question is discussed below.

In the special case when the sonic line is straight the minimum-length nozzle occurs when the initial expansion region on the contour is reduced to a sharp corner at the throat, of angle $\nu_{D/2}$, and the Busemann or straightening part of the contour extends from the throat to the test section. Any streamline within this 'principal' nozzle defines a possible nozzle contour but the singularity at the centre of the expansion wave indicates that the centre of the expansion must lie on or outside the boundary of the flow field. Thus, it is clear that, a streamline outside the principal nozzle cannot be defined.

When the sonic line is curved the minimum-length nozzle becomes more difficult to define. If the principal nozzle is defined to be the streamline passing through the intersection of the branch line with the right-running characteristic through D, as shown by Fig. 4, then the following argument suggests that this defines the minimum-length nozzle of this particular family.

If it can be assumed that a streamline can be defined outside the principal nozzle, then the limit will be reached when the flow possesses a singularity, i.e. when two characteristics intersect as at A in Fig. 4. Then the limiting streamline would be 1–1 through A, and A will represent a sharp-edged corner in the contour. The right-running characteristic through A and D is $\nu + \theta = \nu_D$, and the left-running characteristic through A can be defined as $\nu - \theta = \varepsilon$, where $\varepsilon > 0$. Hence, the Prandtl-Meyer angle and the flow deflection at A are $\frac{1}{2}(\nu_D + \varepsilon)$ and $\frac{1}{2}(\nu_D - \varepsilon)$ respectively.

The flow in the test section must be uniform and parallel to the nozzle axis, thus the contour to the right of A must be shaped so that no reflections occur. Also, section ADC must take the form of a zone of simple waves, because this is the only flow that can be matched to a uniform parallel flow. A simple wave is such that all flow properties along the left-running characteristics are uniform, and since it is undesirable for practical reasons to have compression waves in the nozzle test section, the simple wave must be an expansion wave and hence contour AC must be concave downwards. Hence, along AC the Prandtl-Meyer angle must increase and the flow deflection must decrease.

For a comprehensive account involving the derivation of the equations governing the behaviour of branch lines and limit lines the reader is referred to "Modern Developments in Fluid Dynamics: High Speed Flow", (Clarendon Press) p. 259.

However, as indicated above, at A $\nu_A = \frac{1}{2}(\nu_D + \varepsilon)$, $\theta_A = \frac{1}{2}(\nu_D - \varepsilon)$, and at B where the branch line cuts streamline 1–1, ν_B and θ_B must each be equal to $\nu_{D/2}$. This implies, that along AB, ν decreases and θ increases i.e. a state of affairs exists which violates the conditions stipulated above. Further, it can be seen that these conditions are only satisfied in the region between the nozzle axis and the streamline through the intersection of the branch line and the right-running characteristic through the point on the nozzle axis where the test-section Mach number is first attained.

The nozzle contour at the throat determines the shape of the branch line in the region of the nozzle axis, and thus, if the branch line is made steeper the nozzle length can be reduced still further. This idea leads back to the nozzle which has a straight sonic line at the throat, because the slope of the branch line is then infinite. Hence, it can be concluded that whatever the shape uf the sonic line the principal nozzle is defined as the streamline through the intersection of the branch line and the right-running characteristic through the point on the nozzle axis where the design Mach number is initially attained. This suggests that the absolute minimum-length nozzle occurs when the sonic line is straight. If the sonic line is straight, the velocity gradient at the throat is zero, whereas if the sonic line is curved the velocity gradient is non-zero and positive valued, so that it appears that the design Mach number might possibly be attained in a shorter distance when the gradient is non-zero. At first sight this seems to be a reasonable supposition. Unfortunately, the preceding discussion throws no light at all on its validity and no clear-cut case can be made for supporting or refuting this statement.

2. *The Method of Design of the Inviscid Core.*

2.1. *Region* 1.

To date, very little consideration has been given to the flow in the subsonic part of the nozzle and the wall shape is usually prescribed by any convenient smooth curve. The reasonable flow uniformity achieved with nozzles designed on this basis seems to indicate that the precise shape of the wall is not very important, excepting of course the region immediately upstream of the throat. However, adverse pressure gradients should be avoided as far as possible because these may be strong enough to provoke separation of the boundary layers, and although reattachment is likely to occur upstream of the throat there is the possibility of non-uniformity of the flow downstream of the throat.

It is important, however, to consider the shape of the wall near the throat. Quite a number of design methods have assumed for convenience that the flow is sonic along a straight line normal to the nozzle axis at the throat. Görtler[16] (1939) and Bershader[17] (1949) have shown that this assumption is only valid when the curvature of the wall at the throat is zero. Although this is possible it is difficult to realise in practice. If the curvature were zero any small error in the boundary layer correction would be sufficient to cause a substantial movement of the effective throat.

In the present design the subsonic wall profile was part of a hyperbolic curve having the desired radius of curvature at the throat. This was continued upstream for several times the throat half-height to a station at which the Mach number would be less than about 0·5. On the assumption that conditions further upstream would have little effect on the flow at the throat, this part of the contraction was faired in an arbitrary way to the existing wind-tunnel entry section.

If all lengths are made non-dimensional by dividing them by h, the throat half-height, a system of co-ordinates x and y can be defined, parallel and normal to the nozzle axis respectively. Further, if $x = 0$ is chosen as the location of the throat, when the equation of the nozzle contour is region 1 can be written as:

$$y^2 = 1 + \frac{x^2}{2R} \tag{2.1}$$

2.2. *Region II.*

Some previous designs have been based on a more realistic throat flow with a curved sonic line, but in the main, the theories that have been used are not as accurate as might be desired. Of the various analytic theories that are available it was considered that one due to Hall[1] (1962) was both straightforward to use and sufficiently accurate, so accordingly, it was adopted in the present design. In the original

paper the velocity and flow direction are expressed in terms of x and y as expansions in powers of $1/R$. The results for two-dimensional flow are summarised in Appendix A. However, for nozzle design by the method of characteristics it is more convenient to be able to calculate a particular characteristic, i.e. to know x and y as functions of ν and θ. The necessary inversion has been carried out and the relevant equations are given in Appendix B.

To determine the conditions along the nozzle axis between B and P, the Mach number gradients at these points must be matched to those in regions II and IIIb respectively. The method of characteristics employs ν rather than M, and thus, it is more convenient to work in terms of $\left(\frac{\partial \nu}{\partial x}\right)_{y=0}$ rather than $\left(\frac{\partial M}{\partial x}\right)_{y=0}$. The function $\left(\frac{\partial \nu}{\partial x}\right)_{y=0}$ is defined by equation (A.23) in the vicinity of point B and, in Fig. 3, it has been plotted against ν for various values of R.

2.3. *Region IIIa.*

Initially, the boundary conditions of this region must be specified and these cannot be chosen arbitrarily. The Prandtl-Meyer angle ν must be continuous at B and P and for continuity of wall curvature $\frac{\partial \nu}{\partial x}$ must be continuous. Along the nozzle axis a quadratic variation of ν is the simplest which satisfies these conditions. This can be written in the form

$$\nu - \nu_B = (x - x_B)\left(\frac{\partial \nu}{\partial x}\right)_B + \tfrac{1}{4}(x - x_B)^2 \frac{\left(\frac{\partial \nu}{\partial x}\right)_P^2 - \left(\frac{\partial \nu}{\partial x}\right)_B^2}{\nu_P - \nu_B} \qquad *(2.2)$$

With this variation of ν the length BP is given by

$$x_P - x_B = \frac{2(\nu_P - \nu_B)}{\left(\frac{\partial \nu}{\partial x}\right)_P + \left(\frac{\partial \nu}{\partial x}\right)_B} \qquad (2.3)$$

The flow conditions at P and the characteristic PI, which separates regions IIIa and IIIb, can be calculated directly from the radial flow equations given in Section 2.4.

The flow in region IIIa was calculated by the method of characteristics, and the main equations relevant to this method of calculating two dimensional steady flow are set out in Appendix C. An attempt has been made to assess the errors inherent in the method of characteristics, and a suggestion has been advanced which would reduce the order of magnitude of the errors and cut down amount of labour involved in the calculation of a characteristic network to obtain a given accuracy. This discussion is set out in Appendix D.

2.4. Region *IIIb.*

A plane radial flow is defined as one in which all the dependent variables are a function only of the distance r from a fixed point in the plane. Thus, in region IIIb, the Mach number distribution is given by

$$\frac{r}{r^*} = \frac{1}{M}\left\{\frac{2}{\gamma+1}\left[1+\frac{\gamma-1}{2}M^2\right]\right\}^{\frac{\gamma+1}{2(\gamma-1)}} \qquad (2.4)$$

*In the present design this equation was used in terms of M. The variation of M along the axis was

$$M = 0{\cdot}96338 + 0{\cdot}32324x + 0{\cdot}00609x^2$$

Also, $x_B = 0{\cdot}39001$ and $x_P - x_B = 1{\cdot}58347$

Since the streamlines in region IIIb are straight the boundaries PI and IC can be computed without calculating the region contained within these characteristics. The co-ordinates of any point Q along PI are computed as follows; the flow angle θ_Q is used as a parameter, and from the geometry of the flow the following relations are established

$$x_Q = r^*\left(\frac{r}{r^*}\right)_Q \cos\theta_Q + \left\{x_P - r^*\left(\frac{r}{r^*}\right)_P\right\} \tag{2.8}$$

$$y_Q = r^*\left(\frac{r}{r^*}\right)_Q \sin\theta_Q \tag{2.9}$$

The terms within the brackets in equation (2.8) locate the origin of the radial flow at point 0, see Fig. 2. The value of $(r/r^*)_Q$ is obtained from equation (2.4) and ν_Q, which is given by

$$\nu_Q = \nu_P + \theta_Q$$

from the conditions existing along PI. The co-ordinates of a point R along IC are computed from equations (2.8) and (2.9) with subscript Q replaced by R, and ν_R is defined by

$$\nu_R = \nu_C - \theta_R$$

The values of ν_P and θ_I are fixed by the design Mach number and other properties of the complete nozzle as described in the initial part of this subsection.

2.5. *Region IVa.*

The second matching of the axial Mach number gradient in region IVa is often omitted in designs. However, if the simple wave flow is applied immediately downstream of the inflection point I discontinuities of curvature occur in the nozzle contour at I and K, and the purpose of region IVa is to eliminate these discontinuities. The simplest process to ensure continuity is to define a quadratic distribution of ν along the nozzle axis which satisfies the conditions

$$\nu_D - \nu_C = \Delta\nu = 0(1°)$$

and $\left(\frac{\partial\nu}{\partial x}\right)_C$ as defined by equation (2.5).

The following distribution is suitable†

$$\nu - \nu_D = -\frac{(x - x_D)^2\left(\frac{\partial\nu}{\partial x}\right)_C^2}{4(\nu_D - \nu_C)} \tag{2.10}$$

---

† In the present design M was used as a variable in region IVa. The distribution of M between points C and D was

$$M = -2{\cdot}77449 + 0{\cdot}91315x - 0{\cdot}03610x^2$$

Also, $x_C \doteq 11{\cdot}60854$ and $x_D - x_C = 1{\cdot}03887$

and the corresponding length CD is

$$x_D - x_C = \frac{2(v_D - v_C)}{\left(\frac{\partial v}{\partial x}\right)_C} \tag{2.11}$$

The distribution of v defined by equation (2.10) and the previously computed parameters along the Mach line IC provide sufficient information to calculate the remainder of region IVa by the method of characteristics. Point J is determined by numerical integration of the mass flow across characteristic JD. The process of integration is described in Appendix E.

2.6. *Region IVb.*

To obtain uniform parallel flow at the nozzle test section, the part of the contour downstream of point J must be shaped to prevent the reflection of expansion waves which originate at the walls of the first part of the divergent contour. Because it is adjacent to a region of uniform parallel flow, region IVb must be described by a simple wave flow. Thus, left-running characteristics are by definition straight and the flow properties along such a characteristic are constant. Therefore, if S is a point on the characteristic JD, which is the upstream limit of the simple wave flow, and T is the point where the left-running characteristic through S intersects the nozzle wall

$$x_T - x_S = l_{ST} \cos(\mu + \theta)_S \tag{2.12}$$

$$y_T - y_S = l_{ST} \sin(\mu + \theta)_S \tag{2.13}$$

where l_{ST} is the length ST. By continuity the mass flow across SJ must be equal to the mass flow across ST, i.e.

$$\int_S^J \frac{\rho a \, dy}{\sin(\mu - \theta)} = \rho_S q_S l_{ST} \sin \mu_S$$

Hence

$$l_{ST} = \frac{f(M_S)}{\sin \mu_S} \left\{ (1 - \varepsilon) - \int_0^{y_S} \frac{dy}{Mf(M)\sin(\mu - \theta)} \right\} \tag{2.14}$$

where $f(M)$ is the one-dimensional area ratio function given in equation (2.4) and the integration is along DS. The parametric equations defining the final part of the contour JN are therefore given by substituting for l_{ST} in equations (2.12) and (2.13).

3. *Boundary Layer Correction.*

The nozzle design method described in section 2 can be used to calculate the 'potential outline'. However, in real fluids it is necessary to allow for the growth of the boundary layer along the walls of the tunnel. This is done by displacing the potential outline away from the tunnel centre line, the correction being applied from a knowledge of the displacement thickness of the boundary layers.

There are several approximate methods to predict the rate of boundary-layer growth along the curved walls. These have been summarised by Rogers and Davis[18] (1957). In the present design the boundary layer thickness at the throat was calculated using an expression given by Sibulkin[19] (1956). The rate of growth downstream of the throat was assumed to be constant since this is known to be approximately true and the value of this constant was taken from Rogers and Davis' paper.

Although the assumption is often made that the boundary-layer thickness at the throat is zero, the dimensions of the throat play an important part in the development of the flow. An expression for the boundary-layer thickness at the throat is given by Sibulkin; this can be rewritten in terms of the displacement thickness as

$$\frac{\delta^*\text{throat}}{h} = 0{\cdot}026\left(\frac{R^2}{R_e}\right)^{\frac{1}{5}} \tag{3.1}$$

where

$$R_e = \frac{a^*h}{\nu^*}$$

In order to evaluate R_e, it is first necessary to assign a reasonable value to ν^*. The temperature and therefore the density and viscosity vary across the boundary layer. The pressure, however, remains constant and reduces the problem of choosing appropriate mean values $\bar{\rho}$ and $\bar{\nu}$ to one of choosing $\overline{T}$. As the fifth root of the Reynolds number occurs in equation (3.1) it would appear reasonable, in most cases, to assume that

$$\overline{T} = \frac{T_1 + T_w}{2}$$

where

T_1 = local temperature at edge of boundary layer

T_w = wall temperature

It is difficult to decide conclusively whether or not this assumption is satisfactory. Sibulkin compared the results of his numerical examples with results obtained from other theories. However, his comparisons were only between theories of varying degrees of approximation; consequently the adequacy of the theory could not be satisfactorily judged.

According to Fig. 4 of the paper by Rogers and Davis the mean rate of growth of the boundary-layer displacement thickness $\Delta\delta^*/l$ downstream of the throat for a design Mach number of 3·0 is

$$\frac{\Delta\delta^*}{l} = 0{\cdot}017$$

To compensate for the boundary layers on the side walls Rogers and Davis suggest that the effective displacement of the contour should be $\frac{2h+\omega}{\omega}$ times the displacement thickness, δ^*, on the curved wall, where ω represents the width of the tunnel.

Thus, in the present case, the effective displacement of the potential outline should be 0·0194 inches per inch run, giving a boundary-layer thickness of about 0·28 inches at the run-out position.

4. *The Manufacture and Calibration of the Liner Blocks.*

Two sets of liner blocks were planned in the nozzle design programme. It was decided to manufacture initially a pair of wooden liners which would be used to check the boundary-layer allowance and for carrying out preliminary experiments. The manufacturing tolerances in wood fabrication are unavoidably larger than the desirable tolerances; a second set of metal liner blocks, with satisfactory tolerances are in the stage of manufacture at the time of writing.

The wooden contours were shaped from straight grained obeche which was lengthwise laminated to minimise shrinkage. Co-ordinates of a steel master template were specified for axial intervals of 0·5 inches and ordinates to the nearest 0·01 inches. After preliminary carving the blocks were scraped to fit the template. The finished surface was clear varnished and rubbed down to give a completed surface which was both smooth and hard. To minimise warping the liners were mounted on $\frac{1}{4}$ inch mild steel plates running the whole length of the blocks.

The calibration experiments on these liners showed that the approximate allowance made for the boundary-layer growth was sufficient (see Section 3) and the Mach number distribution in the working section was reasonably uniform, ΔM having a maximum of the order of 0·01. The nozzle calibration is shown in Fig. 6. Static pressure measurements were made on the plane side wall along the nozzle axis and it can be seen that there is good agreement between the experimental and theoretical results. Schlieren photographs of the flow in the test section did not show any wavelets crossing the tunnel.

The specification of the metal liners is much more rigorous for the careful use of an accurate design method is to no avail if the manufacturing tolerances are greatly in excess of the aerodynamic tolerances. Due to the significance of the slope at a point on the contour upon the properties of the flow along the characteristic originating from that point, extreme care in manufacture is necessary to prohibit waviness, or, in the case of very small curvature of the contour, the formation of steps. A simple means of reducing this type of error is to tilt the liner blocks through a finite angle so that all parts of the contour are inclined at an appreciable angle to the milling cutter. The metal liners are being fabricated from aluminium alloy to a maximum tolerance of $\pm 0{\cdot}0002$ inches. Table I gives the co-ordinates of the boundary-layer-corrected nozzle. The surfaces of the completed contours are to be smooth milled and hand finished, and as the supersonic wind tunnel uses dry air as a working fluid it has been decided to leave the liners free of protective treatment.

Acknowledgements.

The author would like to thank Dr. I. M. Hall for the help and encouragement offered in the preparation of this report and the Department of Industrial and Scientific Research for the postgraduate studentship which enabled this work to be carried out.

APPENDIX A

Equations for the Flow in the Region of the Throat

Expressions for the velocity magnitude, q and the flow direction θ in the throat region of a nozzle are given by Hall[1] (1962). If a non-dimensional velocity magnitude $\bar{q}$ is defined by

$$\bar{q} = \frac{q}{a^*} = 1 + q' \tag{A.1}$$

where a^* is the critical speed of sound, Hall's results can be written in the form

$$\bar{q} = 1 + \frac{q_1}{R} + \frac{q_2}{R^2} + \frac{q_3}{R^3} + \ldots . \tag{A.2}$$

$$\theta = \left\{\frac{\gamma+1}{R}\right\}^{\frac{1}{2}} \left\{\frac{\theta_1}{R} + \frac{\theta_2}{R^2} + \frac{\theta_3}{R^3} + \ldots .\right\} \tag{A.3}$$

where R is the ratio of the radius of curvature at the throat to the throat half-height. The q_n's and θ_n's are functions of y and z, the latter being a stretched x co-ordinate defined by

$$x = \left\{\frac{\gamma+1}{R}\right\}^{\frac{1}{2}} z \tag{A.4}$$

The first three coefficients of each series are given in Hall's paper and are reproduced below. These are:

$$q_1 = \frac{1}{2}y^2 - \frac{1}{6} + z \tag{A.5}$$

$$q_2 = \frac{\gamma+6}{18}y^4 - \frac{2\gamma+9}{18}y^2 + \frac{\gamma+30}{270} + \left(y^2 - \frac{1}{2}\right)z - \frac{2\gamma-3}{6}z^2 \tag{A.6}$$

$$\begin{aligned} q_3 = {} & \frac{362\gamma^2+1629\gamma+3357}{12960}y^6 - \frac{194\gamma^2+909\gamma+1737}{2592}y^4 + \\ & + \frac{854\gamma^2+3867\gamma+6939}{12960}y^2 - \frac{732\gamma^2+5523\gamma+22887}{272160} + \\ & + z\left\{\frac{26\gamma^2+75\gamma+285}{288}y^4 - \frac{26\gamma^2+75\gamma+213}{144}y^2 + \right. \\ & \left. + \frac{134\gamma^2+429\gamma+1743}{4320}\right\} + \\ & + z^2\left\{-\frac{3\gamma-2}{4}y^2 + \frac{7\gamma-18}{36}\right\} + \\ & + z^3\left\{\frac{2\gamma^2-33\gamma+9}{72}\right\} \end{aligned} \tag{A.7}$$

and

$$\theta_1 = \frac{1}{6}y^3 - \frac{1}{6}y + yz \tag{A.8}$$

$$\theta_2 = \frac{22\gamma+45}{360}y^5 - \frac{5\gamma+15}{54}y^3 + \frac{34\gamma+165}{1080}y +$$

$$+z\left\{\frac{2\gamma+6}{9}y^3 - \frac{2\gamma+6}{9}y\right\} \tag{A.9}$$

$$\theta_3 = \frac{6574\gamma^2+19257\gamma+18639}{181440}y^7 -$$

$$-\frac{2254\gamma^2+7929\gamma+8739}{25920}y^5 +$$

$$+\frac{5026\gamma^2+21639\gamma+28917}{77760}y^3 -$$

$$-\frac{7570\gamma^2+42735\gamma+74817}{544320}y +$$

$$+z\left\{\frac{362\gamma^2+957\gamma+1107}{2160}y^5 -\right.$$

$$-\frac{194\gamma^2+609\gamma+711}{648}y^3 +$$

$$\left.+\frac{854\gamma^2+3219\gamma+3789}{6480}y\right\} +$$

$$+z^2\left\{\frac{26\gamma^2+3\gamma-15}{144}y^3 - \frac{26\gamma^2+27\gamma+9}{144}y\right\} +$$

$$+z^3\left\{-\frac{\gamma+1}{2}y\right\} \tag{A.10}$$

If $\bar{q}$ is calculated from equation (A.2) the Mach number M, the Mach angle μ and the Prandtl-Meyer angle ν can be computed from

$$M = \sqrt{\frac{2}{\gamma+1}}\bar{q}\left\{1-\lambda^2\bar{q}^2\right\}^{-\frac{1}{2}} \tag{A.11}$$

$$\mu = \sin^{-1}\left(\frac{1}{M}\right) \tag{A.12}$$

and

$$\nu = \frac{1}{\lambda}\tan^{-1}(\lambda\cot\mu) - \tan^{-1}(\cot\mu) \tag{A.13}$$

where

$$\lambda^2 = \frac{\gamma-1}{\gamma+1}$$

For Mach numbers very close to unity it is sometimes more convenient to calculate ν from

$$\nu = (\gamma+1)^{\frac{1}{2}} q'^{\frac{1}{2}} \left\{ \frac{2}{3} q' + \frac{2\gamma-5}{10} q'^2 + \frac{12\gamma^2-28\gamma+39}{112} q'^3 + \ldots . \right\} \tag{A.14}$$

Inserting the series expansion for $\bar{q}$ in equations (A.11), (A.12) and (A.13), the following expansions are obtained:

$$M = 1 + \frac{m_1}{R} + \frac{m_2}{R^2} + \frac{m_3}{R^3} + \ldots . \tag{A.15}$$

$$\mu = \frac{\pi}{2} - \left\{ \frac{\gamma+1}{2} \right\}^{\frac{1}{2}} \left\{ \mu_1 + \frac{\mu_2}{R} + \ldots . \right\} \tag{A.16}$$

$$\nu = \left\{ \frac{\gamma+1}{R} \right\}^{\frac{1}{2}} \left\{ \frac{\nu_1}{R} \quad \frac{\nu_2}{R^2} \quad \frac{\nu_3}{R^3} + \ldots . \right\} \tag{A.17}$$

where

$$m_1 = \frac{\gamma+1}{2} q_1 \tag{A.18}$$

$$\mu_1 = q_1^{\frac{1}{2}} \tag{A.19}$$

$$\nu_1 = \frac{2}{3} q_1^{\frac{3}{2}} \tag{A.20}$$

$$\nu_2 = q_1^{\frac{1}{2}} \left\{ q_2 + \frac{2\gamma-5}{10} q_1^2 \right\} \tag{A.21}$$

$$\nu_3 = q_1^{\frac{1}{2}} \left\{ q_3 + \frac{1}{4}\frac{q_2^2}{q_1} + \frac{2\gamma-5}{4} q_1 q_2 + \frac{12\gamma^2-28\gamma+39}{112} q_1^3 \right\} \tag{A.22}$$

In the matching of region II to region IIIa the function $\left(\frac{\partial v}{\partial x}\right)_{y=0}$ has been used. This can be conveniently written

$$\left(\frac{\partial v}{\partial x}\right)_{y=0} = \frac{dv}{d\mu}\frac{d\mu}{d\bar{q}}\left(\frac{\partial \bar{q}}{\partial z}\right)_{y=0}\left(\frac{dz}{dx}\right) \tag{A.23}$$

where

$$\left(\frac{\partial \bar{q}}{\partial z}\right)_{y=0} = \frac{1}{R}+\frac{1}{R^2}\left\{-\frac{1}{2}-\frac{2\gamma-3}{3}z\right\} + \\ +\frac{1}{R^3}\left\{\frac{134\gamma^2+429\gamma+1743}{4320}+\frac{7\gamma-18}{18}z+\frac{2\gamma^2-33\gamma+9}{24}z^2\right\} \tag{A.24}$$

$$\frac{dv}{d\mu} = \frac{\lambda^2-1}{\tan^2\mu+\lambda^2} \tag{A.25}$$

$$\frac{d\mu}{d\bar{q}} = \frac{-1}{\bar{q}\sqrt{(\bar{q}^2-1)(1-\lambda^2\bar{q}^2)}} \tag{A.26}$$

$$\frac{dz}{dx} = \left\{\frac{R}{\gamma+1}\right\}^{\frac{1}{2}} \tag{A.27}$$

The ratio, Q, of the mass flow through the throat to that calculated by assuming sonic velocity at the plane of the throat is also given by Hall[1] (1962),

$$Q = 1-\varepsilon \\ = 1-\frac{\gamma+1}{R^2}\left\{\frac{1}{90}-\frac{2\gamma+9}{945R}+\frac{334\gamma^2+1703\gamma+2733}{340200R^2}\right\} \tag{A.28}$$

APPENDIX B

The Calculation of a Characteristic in the Throat Region

The values of θ and ν at selected points just downstream of the throat could be calculated from the equations given in Appendix A and these values used to start the calculation of region IIIa. In general, however, these values would not be rounded numbers and interpolation of tables would be necessary at each stage of the calculation. A more convenient approach is to invert the equations so that the co-ordinates of a point at which specific values of θ and ν have been chosen can be obtained directly. If suitably rounded values of θ and ν are taken it is possible to use existing tables of characteristic slopes directly.

The process of inversion to obtain y and z as functions of ν and θ is not straightforward. The series for ν given in equation (A.17) is not convergent near the sonic line, e.g. q_1 occurs in the denominator of equation (A.22). At first sight it appears that this difficulty can be surmounted by using equation (A.2) in place of equation (A.17) and expressing y and z as functions of $\bar{q}$ and θ. This inversion is straightforward in principle and the method of solution was identical to that detailed below. Unfortunately, the series expressions obtained were not convergent in the region of the branch line. A pointer to the method eventually used was found by investigating the reasons underlying the difficulty occurring in the first attempt. In this case the objection arose from the incorrect expansion of ν near the sonic line. In the vicinity of the sonic line it is possible for ν to be real even though ν_1 is imaginary. This suggested that the function $\eta = \nu^2$ might be more appropriate since it is a real and unique function of $\bar{q}$ at both subsonic and supersonic speeds.

The series for θ and η were inverted as follows. Squaring equation (A.14) and substituting for $\bar{q}$ from equation (A.2) gives

$$\eta = (\gamma+1)\left\{\frac{\eta_1}{R^3}+\frac{\eta_2}{R^4}+\frac{\eta_3}{R^5}+\ldots.\right\} \tag{B.1}$$

where

$$\eta_1 = \frac{4}{9}q_1^3 \tag{B.2}$$

$$\eta_2 = \frac{4}{3}q_1^2\left\{q_2+\frac{2\gamma-5}{10}q_1^2\right\} \tag{B.3}$$

$$\eta_3 = q_1\left\{\frac{4}{3}q_2^2+\frac{4}{3}q_1\,q_3+\frac{8(2\gamma-5)}{15}q_1^2\,q_2+\frac{96\gamma^2-280\gamma+375}{525}q_1^4\right\} \tag{B.4}$$

Thus, the equations to be inverted are (A.3) and (B.1). To a first approximation, these equations reduce to

$$\eta_1(y,z) = \frac{R^3\eta}{(\gamma+1)} \tag{B.5}$$

$$\theta_1(y,z) = \frac{R^{\frac{3}{2}}\theta}{(\gamma+1)^{\frac{1}{2}}} \tag{B.6}$$

The right hand sides of both equations (B.5) and (B.6) are constant and known quantities. It is convenient therefore to introduce P and Q where

$$Q = \left\{ \frac{9\,R^3\eta}{4(\gamma+1)} \right\}^{\frac{1}{3}}$$

$$P = \frac{R^{\frac{3}{2}}\theta}{(\gamma+1)^{\frac{1}{2}}}$$

A further substitution,

$$t = z - \frac{1}{6}$$

reduces equations (B.5) and B.6) to

$$\frac{1}{2}y^2 + t = Q \tag{B.7}$$

$$\frac{1}{6}y^3 + yt = P \tag{B.8}$$

from which t can be eliminated to give a cubic equation for y, i.e.

$$y^3 - 3Q_1 y + 3P = 0 \tag{B.9}$$

The number of real roots of this equation depends upon the sign of the discriminant. A function D which is proportional to the discriminant is given by

$$D = \frac{9}{4}P^2 - Q^3 = \frac{9R^3}{4(\gamma+1)}(\theta^2 - \eta) \tag{B.10}$$

Hence, the solution of equation (B.9) can be given in one of the following ways, depending on the sign of D.

(i) $D > 0$, i.e. $|\theta| > v$. There is only one real root which is given by

$$y = \left(D^{\frac{1}{2}} - \frac{3P}{2}\right)^{\frac{1}{3}} - \left(D^{\frac{1}{2}} + \frac{3P}{2}\right)^{\frac{1}{3}} \tag{B.11}$$

where the positive root of D is used. If P is positive the corresponding point in the x, y plane lies in the lower half plane between the sonic line and the left-running characteristic from the sonic point on the axis, as shown in Fig. 7. For negative P the solution lies in the corresponding segment in the upper half plane i.e. the mirror image in the x-axis.

(ii) $D = 0$, i.e. $|\theta| = v$. There are two coincident real roots and one distinct real root. The latter is

$$y = \mp 2Q^{\frac{1}{2}} \tag{B.12}$$

and the double root is

$$y = \pm Q^{\frac{1}{2}} \tag{B.13}$$

where the upper signs are taken when P is positive, and the lower when P is negative. The double root corresponds to a point on the branch line and the single root to a point on the left-running characteristic through the sonic point on the x-axis.

(iii) $D<0$, i.e. $|\theta|<\nu$. There are three distinct real roots given by

$$y = 2Q^{\frac{1}{2}}\cos(\theta+120i) \tag{B.14}$$

where

$$\cos 3\theta = -\frac{3P}{2Q^{\frac{3}{2}}} \tag{B.15}$$

the positive square root being taken in both equations. When P is positive, two of the solutions lie in the upper half plane on the same right-running characteristic, one on either side of the branch line. The third root lies in the lower half plane in the narrow sector between the left-running characteristic through the sonic point on the x-axis and the line $\theta = 0$. The locations of roots for all three cases when $P>0$ are illustrated in Fig. 7.

It should be noted that any roots which lie outside the range $|y|>1{\cdot}0$ are valid, because this discussion is essentially mathematical and does not recognise the practical limits imposed by the nozzle contour.

Several tables are available which enable the roots of equation (B.9) to be found directly. For example, if the tables given by Neumark[20] (1962) are used the equation has to be written in the standard form

$$4s^3-3s = \Delta$$

which requires the substitution

$$y = 2Q^{\frac{1}{2}}s$$

The parameter Δ, against which roots are tabulated, is given by

$$\Delta = -\frac{3P}{2Q^{\frac{3}{2}}}$$

It is now assumed that the solutions of equations (B.7) and (B.8) are y_0 and t_0. The complete solutions can be written in the form

$$y = y_0+\frac{y_1}{R}+\frac{y_2}{R^2}+\ldots. \tag{B.16}$$

$$t = t_0+\frac{t_1}{R}+\frac{t_2}{R^2}+\ldots. \tag{B.17}$$

where $y_1, y_2, \ldots. t_1, t_2, \ldots.$ are conveniently expressed in terms of y_0 and t_0. Pairs of simultaneous equations for y_i and t_i can be obtained by expanding equations (A.3) and (B.1) and collecting the coefficients of each power of R. These are of the form:

$$y_i\left(\frac{\partial\eta_1}{\partial y}\right)_0+t_i\left(\frac{\partial\eta_1}{\partial t}\right)_0+N_i = 0 \tag{B.18}$$

$$y_i\left(\frac{\partial\theta_1}{\partial y}\right)_0+t_i\left(\frac{\partial\theta_1}{\partial t}\right)_0+\Theta_i = 0 \tag{B.19}$$

where

$$N_1 = \eta_2$$

$$\Theta_1 = \theta_2$$

$$N_2 = \frac{y_1^2}{2}\frac{\partial^2\eta_1}{\partial y^2}+\frac{t_1^2}{2}\frac{\partial^2\eta_1}{\partial t^2}+y_1t_1\frac{\partial^2\eta_1}{\partial y.\partial t}+y_1\frac{\partial\eta_2}{\partial y}+t_1\frac{\partial\eta_2}{\partial t}+\eta_3$$

$$\Theta_2 = \frac{y_1^2}{2}\frac{\partial^2\theta_1}{\partial y^2}+\frac{t_1^2}{2}\frac{\partial^2\theta_1}{\partial t^2}+y_1t_1\frac{\partial^2\theta_1}{\partial y.\partial t}+y_1\frac{\partial\theta_2}{\partial y}+t_1\frac{\partial\theta_2}{\partial t}+\theta_3$$

all terms being evaluated at (y_0, t_0). The solutions of simultaneous equations (B.18) and (B.19) are

$$y_i = \nabla^{-1}\left\{\Theta_i\frac{\partial\eta_1}{\partial t}-N_i\frac{\partial\theta_1}{\partial t}\right\} \tag{B.20}$$

$$t_i = \nabla^{-1}\left\{N_i\frac{\partial\theta_1}{\partial y}-\Theta_i\frac{\partial\eta_1}{\partial y}\right\} \tag{B.21}$$

where

$$\nabla = \left(\frac{\partial\eta_1}{\partial y}\right)_0\left(\frac{\partial\theta_1}{\partial t}\right)_0-\left(\frac{\partial\theta_1}{\partial y}\right)_0\left(\frac{\partial\eta_1}{\partial t}\right)_0 \tag{B.22}$$

$$= \frac{4}{3}q_1^2\ \frac{1}{2}y_0^2-t_0$$

For $i = 1$ the solutions of equations (B.20) and (B.21) become

$$y_1 = y_0\left\{\frac{\gamma+3}{9}-\frac{8\gamma+15}{90}y_0^2-\frac{2\gamma}{15}t_0\right\} \tag{B.23}$$

$$t_1 = \frac{2\gamma-15}{360}-\frac{2\gamma+5}{120}y_0^4-\frac{2\gamma+15}{30}y_0^2t_0+\frac{\gamma+3}{9}t_0+\frac{2\gamma}{15}t_0^2 \tag{B.24}$$

In view of the complexity of the algebra it was decided to calculate y_2 and t_2 numerically for a particular value of γ. For $\gamma = 1{\cdot}4$, the results are

$$y_2 = y_0\{(0{\cdot}0254\,y_0^4-0{\cdot}2476)+t_0(-0{\cdot}1554\,y_0^2+ \tag{B.25}$$

$$+0{\cdot}7622)+0{\cdot}8843\,t_0^2\}$$

$$t_2 = (-0{\cdot}0262\,y_0^6+0{\cdot}0746\,y_0^4+0{\cdot}0098)+$$

$$+t_0(-0{\cdot}0176\,y_0^4+0{\cdot}1356\,y_0^2-0{\cdot}2478)+$$

$$+t_0^2(-0{\cdot}2748\,y_0^2+0{\cdot}5177)+0{\cdot}3505\,t_0^3 \tag{B.26}$$

For $i = 1$ and 2, the factor ∇ has been extracted from the numerator so that the question of convergence of these functions in the region where $t_0 \simeq \frac{y_0^2}{2}$ does not arise. Along the branch line $t_0 = \frac{y_0^2}{2}$, however, and the problem is trivial in solution because $|\theta| = v$.

APPENDIX C

Equations for the Method of Characteristics

The main equations necessary for the solution of a two-dimensional, isentropic, steady supersonic flow by the method of characteristics are set out below. The characteristics are defined by the following equations

$$\frac{dy}{dx} = \tan(\mu+\theta) \tag{C.1}$$

$$\frac{dy}{dx} = -\tan(\mu-\theta) \tag{C.2}$$

for left-running and right-running characteristics respectively. Along a left-running characteristic

$$\nu-\theta = \propto = \text{constant} \tag{C.3}$$

and along a right-running characteristic

$$\nu+\theta = \beta = \text{constant} \tag{C.4}$$

Fig. 8 shows a sketch of a typical characteristic mesh. It is assumed that conditions at co-ordinates (x_1, y_1) and (x_2, y_2) are known and (x_3, y_3), which lies at the intersection of the characteristics $\nu+\theta = \beta_2$ and $\nu-\theta = \propto_1$, is the point that it is desired to compute. Using this figure, equations (C.1) and (C.2) can be replaced by

$$\frac{y_3-y_1}{x_3-x_1} = m_{13} \tag{C.5}$$

$$\frac{y_3-y_2}{x_3-x_2} = -m_{23} \tag{C.6}$$

where m_{13} and m_{23} are mean values of $\tan(\mu+\theta)$ and $\tan(\mu-\theta)$ suitably defined in the relevant intervals; a discussion on the best values to use is given below.

Equations (C.5) and (C.6) can easily be solved for x_3 and y_3. It appears, however, that the expressions given in most textbooks are not in their most satisfactory form. The following scheme is suggested since fewer significant figures need be used in the calculations;

$$\Delta x = x_2-x_1 \tag{C.7}$$

$$\Delta y = y_2-y_1 \tag{C.8}$$

$$\delta = \frac{\Delta y+m_{23}\Delta x}{m_{13}+m_{23}} \tag{C.9}$$

giving

$$x_3 = x_1+\delta \tag{C.10}$$

$$y_3 = y_1+m_{13}\delta \tag{C.11}$$

In general, to estimate m_{13}, three simple methods are recommended*. These are

(i) $$m_{13} \simeq \tan\left\{\frac{1}{2}(\mu_1+\theta_1)+\frac{1}{2}(\mu_3+\theta_3)\right\} \tag{C.12}$$

which corresponds to replacing the exact characteristic by a circular arc,

(ii) $$m_{13} \simeq \frac{1}{2}\left\{\tan(\mu_1+\theta_1)+\tan(\mu_3+\theta_3)\right\} \tag{C.13}$$

which is equivalent to integrating equation (C.1) using the trapezium rule, and

(iii) $$m_{13} \simeq \tan(\mu+\theta)_m \tag{C.14}$$

where the subscript of 'm' refers to the value of $(\mu+\theta)$ at the point where

$$\beta = \frac{1}{2}\left\{\beta_1+\beta_3\right\}$$

The last method, suggested by Temple[21] (1944), is the most convenient in some respects, and trial calculations using the exact solution for a radial source flow as a comparison show that it appears to give slightly better results than the other two. In mathematical terms, however, the three estimates are all of the same order of accuracy and there is no *priori* reason why anyone of them should be the most appropriate in any particular case.

Equation (C.12) cannot be used in conjunction with tables of characteristic slopes and is therefore discarded at this stage. Further consideration of the other two estimates is given below.

Estimates of the mean value of $\tan(\mu+\theta)$ between the points (x_1, y_1) and (x_3, y_3), in Fig. 8, can be obtained by integrating equation (C.1) using standard finite difference formulae. Putting

$$f(x) = \tan(\mu+\theta) = \tan\omega \tag{C.15}$$

equation (C.1) gives

$$y_3-y_1 = \int_{x_1}^{x_3} f(x)dx \tag{C.16}$$

$$= \frac{\delta}{2}\left\{f(x_1)+f(x_3)\right\} + \delta^3 L + O(\delta^5) \tag{C.17}$$

where

$$L = -\frac{1}{24}\left\{f^{11}(x_1)+f^{11}(x_3)\right\} \tag{C.18}$$

$$= -\frac{1}{12}f^{11}(\bar{x}) + O(\delta^2) \tag{C.19}$$

and $\bar{x}$ is the arithmetic mean of x_1 and x_3. The derivatives are taken along the characteristic. Equation (C.17) shows that the error in m_{13} as given by equation (C.13) is $O(\delta^2)$ or, to be more precise, $\delta^2 L$.

*A similar argument also applies to m_{23}.

An alternative approach is to rewrite equation (C.16) as

$$y_3 - y_1 = \int_{\beta_1}^{\beta_3} g(\beta)\, d\beta \tag{C.20}$$

where

$$g(\beta) = f(x)\frac{dx}{d\beta} = \tan\omega \frac{dx}{d\beta} \tag{C.21}$$

Hence,

$$y_3 - y_1 = \sum g(\beta_m) + \frac{\Sigma^3}{24} g^{11}(\beta_m) + O(\Sigma^5) \tag{C.22}$$

where

$$\Sigma = \beta_3 - \beta_1 \tag{C.23}$$

and β_m is the arithmetic mean of β_1 and β_3. The variables x and β can be related by

$$\delta = \Sigma \left(\frac{dx}{d\beta}\right)_m + \frac{\Sigma^3}{24}\left(\frac{d^3x}{d\beta^3}\right)_m + O(\Sigma^5) \tag{C.24}$$

where subscript 'm' refers to values taken at β_m. Equation (C.22) can be re-written

$$y_3 - y_1 = \delta \tan\omega + \delta^3 M + O(\delta^5) \tag{C.25}$$

where

$$M = \frac{1}{24}\left(\frac{dx}{d\beta}\right)_m^{-3} \left\{ g^{11}(\beta_m) - \tan\omega_m \left(\frac{d^3x}{d\beta^3}\right)_m \right\} \tag{C.26}$$

Equation (C.25) shows that the error in m_{13} as given by equation (C.14) is also of $O(\delta^2)$.

APPENDIX D

A Method to Reduce the Error in the Mean Slope of a Characteristic

D.1. Estimation of Mean Slope at a General Point.

It has been shown above that for given values of x_1 and x_3 the error in y_3 is $O(\delta^3)$. In practice, x_3 is unknown and is determined from the starting conditions at (x_1, y_1) and (x_2, y_2). It is easily seen, however, that the resultant errors in x_3 and y_3 are still $O(\delta^3)$; a detailed discussion is given by Hall[22] (1956). In many cases these errors are small enough to be of no importance but they can be quite significant, particularly when the Mach number is close to unity. When the errors are thought to be significant the standard method of checking is to repeat the calculation with a step size equal to half the original one, and to repeat the process until successive calculations give the same result to the accuracy required. However, this process is rather unsatisfactory because it converges only slowly. Halving the step size approximately quadruples the number of steps in the characteristic mesh so that the final error is only slightly less than half the original one. It would seem worth while, therefore, to develop a method which would reduce the order of magnitude of the error; this has been done by combining two of the estimates for m_{13} in such a way that the terms of $O(\delta^3)$ are eliminated.

To combine equation (C.17) and (C.25) a function ϕ is introduced which is dependent upon the conditions that exist along a particular characteristic. Multiplying equation (C.17) by $(1-\phi)$, equation (C.25) by ϕ and adding the results gives

$$y_3 - y_1 = \delta \left\{ (1-\phi)\frac{\tan\omega_1 + \tan\omega_3}{2} + \phi \tan\omega_m \right\}$$

$$+\delta^3\{(1-\phi)L + \phi M\} + O(\delta^5) \tag{D.1}$$

Therefore, if ϕ is chosen so that

$$(1-\phi)L + \phi M = 0 \tag{D.2}$$

an estimate of m_{13} can be obtained which is in error by $O(\delta^4)$, i.e.

$$m_{13} \simeq (1-\phi)\frac{\tan\omega_1 + \tan\omega_3}{2} + \phi \tan\omega_m \tag{D.3}$$

Substituting in equation (D.2) from equations (C.19) and (C.26) gives, after some reduction,

$$\phi = \frac{2}{3}\left\{ 1 - \frac{\dfrac{df}{d\beta}\cdot\dfrac{d^2x}{d\beta^2}}{\dfrac{dx}{d\beta}\cdot\dfrac{d^2f}{d\beta^2}} \right\} \tag{D.4}$$

where $f(x) = \tan\omega$ and the derivatives are evaluated at the mid-point of the interval. In general, calculations are made at equal intervals of β so that the differential terms can be easily evaluated. Along any characteristic it can be shown that

$$\frac{d\omega}{d\beta} = \frac{1}{2}\frac{\tan^2\mu + 2\lambda^2 - 1}{\lambda^2 - 1} \tag{D.5}$$

and

$$\frac{d^2\omega}{d\beta^2} = \frac{\tan\mu\sec^2\mu(\tan^2\mu+\lambda^2)}{2(\lambda^2-1)^2} \tag{D.6}$$

Thus, functions dependent upon equations (D.5) and (D.6), e.g. $\frac{df}{d\beta}$ and $\frac{d^2f}{\beta^2}$, can be evaluated without knowing the space co-ordinates of a characteristic mesh.

The calculation of ϕ increases the time required for each stage of a characteristic mesh but this is offset to some extent because relatively large step sizes may be used. It is estimated that the total time required to compute a characteristic network to a given accuracy can be as little as one sixth of the time required when the first approximation to m_{13} is used.

D.2. Estimation of Mean Slope near a Branch Line.

In cases where a branch line exists in the flow field allowance can be made in the computations by using a similar procedure to that described above. If the branch line is a left-running characteristic no allowance is necessary along left-running characteristics. However, m_{23} has a maximum on each right-running characteristic where it crosses the branch line and the mean value given in section D.1 is inappropriate.

Consider a section of the characteristic network as shown in Fig. 8 but such that the 1–3 characteristic is now a branch line. Then, because m_{23} has a maximum at (x_3, y_3),

$$f(x) = f(x_3)+\frac{(x-x_3)^2}{2}\left(\frac{d^2f}{dx^2}\right)_3+\frac{(x-x_3)^2}{6}\left(\frac{d^3f}{dx^3}\right)_3+O(\delta^4) \tag{D.7}$$

Hence,

$$y_3-y_2 = \int_{x_2}^{x_3} f(x)dx \tag{D.8}$$

$$= \delta f(x_3)+\frac{\delta^3}{6}\left(\frac{d^2f}{dx^2}\right)_3-\frac{\delta^4}{24}\left(\frac{d^3f}{dx^3}\right)_3+O(\delta^5) \tag{D.9}$$

where

$$\delta = x_3-x_2$$

But,

$$f(x_2) = f(x_3)+\frac{\delta^2}{2}\left(\frac{d^2f}{dx^2}\right)_3-\frac{\delta^3}{6}\left(\frac{d^3f}{dx^3}\right)_3+O(\delta^4) \tag{D.10}$$

so that the term of $O(\delta^3)$ in equation (D.9) can be eliminated giving

$$y_3-y_2 = \frac{\delta}{3}\left\{\tan\omega_2+2\tan\omega_3\right\}+\delta^4L+O(\delta^5) \tag{D.11}$$

where

$$L = \frac{1}{72}\left(\frac{d^3 f}{dx^3}\right)_3 \tag{D.12}$$

Thus, to a first approximation

$$m_{23} = \frac{1}{3}\left\{\tan\omega_2 + 2\tan\omega_3\right\} \tag{D.13}$$

To obtain the relevant form of "Temple's method" account is taken of the fact that the characteristic co-ordinate $\propto$ has a minimum at x_3 i.e.

$$\propto = \propto_3 + \frac{(x-x_3)^2}{2}\left(\frac{d^2\propto}{dx^2}\right)_3 + \frac{(x-x_3)^2}{6}\left(\frac{d^3\propto}{dx^3}\right)_3 + O(\delta^4) \tag{D.14}$$

Writing

$$\begin{aligned} f(x) &= F(\propto) \\ &= F(\propto_3) + (\propto - \propto_3)\left(\frac{dF}{d\propto}\right)_3 + O(\Sigma^2) \end{aligned} \tag{D.15}$$

where

$$\Sigma = \propto_2 - \propto_3$$

equation (D.14) can be used to give

$$\begin{aligned} f(x) = F(\propto_3) &+ \frac{(x-x_3)^2}{2}\left(\frac{d^2\propto}{dx^2}\right)_3\left(\frac{dF}{d\propto}\right)_3 + \\ &+ \frac{(x-x_3)^3}{6}\left(\frac{d^3\propto}{dx^3}\right)_3\left(\frac{dF}{d\propto}\right)_3 + O(\delta^4) \end{aligned} \tag{D.16}$$

Hence,

$$\begin{aligned} y_3 - y_2 = \delta F(\propto_3) &+ \frac{\delta^3}{6}\left(\frac{d^2\propto}{dx^2}\right)_3\left(\frac{dF}{d\propto}\right)_3 \\ &+ \frac{\delta^4}{24}\left(\frac{d^3\propto}{dx^3}\right)_3\left(\frac{dF}{d\propto}\right)_3 + O(\delta^5) \end{aligned} \tag{D.17}$$

If a constant ζ $(0 < \zeta < 1)$ is introduced such that

$$F(\propto_3 + \Sigma) = F(\propto_3) + \Sigma\left(\frac{dF}{d\propto}\right)_3 + O(\Sigma^2) \tag{D.18}$$

$$\begin{aligned} &= F(\propto_3) + \frac{\delta^2}{2}\left(\frac{d^2\propto}{dx^2}\right)_3\left(\frac{dF}{d\propto}\right)_3 + \\ &+ \frac{\delta^3}{6}\left(\frac{d^3\propto}{dx^3}\right)_3\left(\frac{dF}{d\propto}\right)_3 + O(\delta^4) \end{aligned} \tag{D.19}$$

then equation (D.17) can be written

$$y_3 - y_2 = \delta F(\propto_3 + \quad \Sigma) + \frac{\delta^3}{6}\left(\frac{d^2\propto}{dx^2}\right)_3\left(\frac{dF}{d\propto}\right)_3(1-3 \quad) +$$

$$+\frac{\delta^4}{24}\left(\frac{d^3\propto}{dx^3}\right)_3\left(\frac{dF}{d\propto}\right)_3(1-4 \quad) + O(\delta^5) \tag{D.20}$$

The term of $O(\delta^3)$ can be eliminated by choosing

$$= \frac{1}{3}$$

so that

$$y_3 - y_2 = \delta F\left(\propto_3 + \frac{\Sigma}{3}\right) + \delta^4 M' + O(\delta^5) \tag{D.21}$$

where

$$M' = -\frac{1}{72}\left(\frac{d^3\propto}{dx^3}\right)_3\left(\frac{dF}{d\propto}\right)_3 \tag{D.22}$$

Hence, to a first approximation,

$$m_{23} = \tan\left\{\frac{2\omega_3 + \omega_2}{3}\right\} \tag{D.23}$$

In a similar manner to that described above the two first approximations can be combined so that the error terms of the highest order are eliminated. Introducing ψ, in place of the original function ϕ, an identical procedure gives

$$m_{23} = \frac{1-\psi}{3}\left\{\tan\omega_2 + 2\tan\omega_3\right\} + \psi\tan\left\{\frac{\omega_2 + 2\omega_3}{3}\right\} \tag{D.24}$$

where

$$\psi = \frac{\dfrac{d^3\omega}{dx^3}}{\dfrac{d^3\omega}{dx^3} + \dfrac{d\omega}{d\propto}\dfrac{d^3\propto}{dx^3}} \tag{D.25}$$

the derivatives being evaluated at the branch line. Since $\dfrac{d\propto}{dx} = 0$ at the branch line, this equation reduces to

$$\psi = \frac{1}{2} \tag{D.26}$$

Therefore equation (D.24) becomes

$$m_{23} = \frac{1}{6}\left\{\tan\omega_2 + 2\tan\omega_3\right\}\frac{1}{2}\tan\left\{\frac{\omega_2 + 2\omega_3}{3}\right\} \tag{D.27}$$

APPENDIX E

Determination of the Nozzle Contour by Integrating along a Characteristic

The nozzle contour in regions IIIa and IVa is determined by equating the mass flow across a characteristic to the mass flow through the throat. The mass flow across a characteristic, made non-dimensional by dividing by the mass flow calculated from one-dimensional considerations, is Q_1 where

$$Q_1(y) = \int_0^y W dy \tag{E.1}$$

and along a right-running characteristic,

$$W = \frac{\rho a \operatorname{cosec}(\mu - \theta)}{\rho^* a^*} \tag{E.2}$$

An equivalent form which is more convenient for calculation is

$$W = \{Mf(M)\sin(\mu - \theta)\}^{-1} \tag{E.3}$$

where $f(M)$ is the one-dimensional area ratio defined by

$$f(M) = \frac{1}{M}\left\{\frac{2}{\gamma+1}\left(1+\frac{\gamma-1}{2}M^2\right)\right\}^{\frac{\gamma+1}{2(\gamma-1)}} \tag{E.4}$$

and tabulated in detail by Riise[23] (1953) and others. The function W can be evaluated at each point of the characteristic network and Q_1 can be obtained at these points by numerical integration. In general the trapezium rule is not sufficiently accurate for the evaluation of Q_1 from equation (E.1) and recourse must be made to more refined integration formulae. Some suitable formulae for unequal intervals of Δy have been derived by Hartley[24] (1953); the required formula when W is given at y_1, y_2 and y_3 is

$$\int_{y_1}^{y_3} W dy = \frac{y_3 - y_1}{6}\left\{K_1 W_1 + K_2 W_2 + K_3 W_3\right\} \tag{E.5}$$

where

$$K_1 = 2 - \Gamma \tag{E.6}$$

$$K_2 = 2 + \Gamma + \Gamma^{-1} \tag{E.7}$$

$$K_3 = 2 - \Gamma^{-1} \tag{E.8}$$

and

$$\Gamma = \frac{y_3 - y_2}{y_2 - y_1} \tag{E.9}$$

An equivalent formula for calculating the integral over one interval of Δy can be derived. This is

$$\int_{y_2}^{y_3} W dy = \frac{y_3 - y_2}{6} \left\{ K_1 W_1 + K_2 W_2 + K_3 W_3 \right\} \tag{E.10}$$

where, with Γ defined as above

$$K_1 = -\frac{\Gamma^2}{1+\Gamma} \tag{E.11}$$

$$K_2 = \Gamma + 3 \tag{E.12}$$

$$K_3 = \frac{3+2\Gamma}{1+\Gamma} \tag{E.13}$$

The ratio of the mass flow through the throat to the mass flow obtained by one-dimensional considerations is Q, where Q is given by equation (A.28); for $R = 5{\cdot}0$

$$Q = 0{\cdot}99911 \tag{E.14}$$

Therefore, y_ω, the value of y at the point where the characteristic intersects the nozzle contour is given

$$Q_1(y_\omega) = 0{\cdot}99911 \tag{E.15}$$

The value of y_ω is found by interpolation; again, great care must be taken to avoid a significant loss of accuracy. Suppose, for example, that Q_1 attains the required value between points S and T on the characteristic. Then y, Q_1 and $\frac{Q_1}{dy} = W$ are known at both points, enabling a cubic variation of y with Q to be defined in the interpolation region. The equation to this cubic can be written

$$y = y_S + \left(\frac{dy}{dQ_1}\right)_S (Q_1 - Q_{1_S}) + B(Q_1 - Q_{1_S})^2 + C(Q_1 - Q_{1_S})^3 \tag{E.16}$$

where

$$B = \frac{1}{(Q_{1_T} - Q_{1_S})^2} \left\{ 3(y_T - y_S) - (Q_{1_T} - Q_{1_S}) \left[2\left(\frac{dy}{dQ_1}\right)_S + \left(\frac{dy}{dQ_1}\right)_T \right] \right\} \tag{E.17}$$

and

$$C = \frac{1}{(Q_{1_T} - Q_{1_S})^3} \left\{ -2(y_T - y_S) + (Q_{1_T} - Q_{1_S}) \left[\left(\frac{dy}{dQ_1}\right)_S + \left(\frac{dy}{dQ_1}\right)_T \right] \right\} \tag{E.18}$$

In the region near the throat W is approximately equal to unity and it is convenient to work with the function k where

$$k = 1 - W \tag{E.19}$$

This step reduces the number of significant figures in each calculation. Using this function, equation (E.1) becomes

$$y_\omega - Q_1(y_\omega) = \int_0^{y_w} k\,dy \tag{E.20}$$

Another function Q_2 is defined by

$$Q_2 = \int_0 k\,dy = y - \int_0 W dy \tag{E.21}$$

Therefore,

$$\frac{dQ_2}{dQ_1} = \frac{k}{1-k} \tag{E.22}$$

and

$$\frac{d^2Q_2}{dQ_1^2} = \frac{\dfrac{dk}{dy}}{(1-k)^3} \tag{E.23}$$

It is therefore possible to use the known value of Q_2 and $\frac{Q_2}{dQ_1}$ at each end of each interval to prescribe a cubic variation of Q_2 as a function of Q_1 and, hence, to find the value of Q_2 at which $Q_1 = 0{\cdot}99911$. If either of the points S or T lies on the branch line a further condition can be stipulated. Along any right-running characteristic, v has a minimum at the branch line. From equation (E.3) it can be shown that the function k also has a minimum at this point. Hence, equation (E.23) shows that at the branch line the variation of Q_2 with Q_1 has an inflection point. This enables a quartic variation of Q_2 as a function of Q_1 to be prescribed and Q_2 determined at the point where $Q_1 = 0{\cdot}99911$.

SYMBOLS

a	Speed of sound
A	Cross-sectional area
D	Function dependent upon discriminant of equation (B.9)
h	Throat half height
k	Defined by equation (E.19)
l	Distance measured along nozzle axis between throat and nozzle run out position
l_{ST}	Length along a characteristic in the simple wave flow region
L	Defined by equation (C.19)
L'	Defined by equation (D.12)
m_{13}, m_{23}	Mean values of $\tan(\mu+\theta)$ and $\tan(\mu-\theta)$ respectively
M	Defined by equation (C.26)
M'	Defined by equation (D.22)
M	Mach number
N	Defined by equation (B.18)
P	$\dfrac{R^{\frac{3}{2}}\theta}{(\gamma+1)^{\frac{1}{2}}}$
q	Velocity magnitude
$\bar{q}, q'$	Defined by equation (A.1)
Q	$\left\{ \dfrac{9R^3\eta}{4(\gamma+1)} \right\}^{\frac{1}{3}}$
Q	Ratio of the mass flow through the throat to that calculated by assuming sonic velocity at the plane of the throat
Q_1	Ratio of the mass flow across a characteristic to that calculated by assuming sonic velocity at the plane of the throat
Q_2	Defined by equation (E.21)
r	Radial distance from source point in radial flow
R	Ratio of radius of curvature at throat to the throat half height
R_e	Reynolds number
s	$\dfrac{y}{2Q^{\frac{1}{2}}}$
t	$z-\dfrac{1}{6}$
ω	Width of supersonic tunnel
W	Defined by equation (E.2)
x, y	Two-dimensional Cartesian co-ordinates

SYMBOLS—*continued*

$\bar{x}$	Arithmetic mean of x_1 and x_3
z	$\left\{ \frac{R}{\gamma+1} \right\}^{\frac{1}{2}} x$
α	Constant of integration for a left-running characteristic
β	Constant of integration for a right-running characteristic
γ	Ratio of specific heats
Γ	Defined by equation (E.9)
δ	$x_3 - x_1$ a measure of the step size in a characteristic network
Δ	$-\frac{3P}{2Q^{\frac{1}{2}}}$
∇	Defined by equation (B.22)
δ_1	Boundary layer thickness
δ^*	Boundary Layer displacement thickness
ε	$1-Q$
Σ	$\beta_3 - \beta_1$ a measure of the step size in a characteristic network
λ^2	$\frac{\gamma-1}{\gamma+1}$
θ	Flow deflection relative to nozzle axis
Θ	Defined by equation (B.19)
η	v^2, defined by equation (B.1)
ρ	Fluid density
μ	Mach angle
ν	Prandtl-Meyer angle
ω	Inclination of a characteristic to the nozzle axis
ϕ	Defined by equation (D.4)
ψ	Defined by equation (D.25)

The following symbols are used to represent points in the flow field and also as subscripts to denote the value of a flow variable at a particular point:

B, P, C, D	Intersection points of certain left-running and right-running characteristics with the nozzle axis
I	Conditions at the inflection point
Q, R	Upstream and downstream end points, respectively, on a radial flow streamline (Fig. 2)
S, T	Upstream and downstream end points, respectively, of a characteristic crossing the simple wave flow region (Fig. 2)

SYMBOLS—*continued*

subscripts:

ω	Conditions along the contour
m	Arithemetic mean

superscript:

*	Conditions at throat

REFERENCES

No.	*Author(s)*	*Title, etc.*
1	I. M. Hall	Transonic flow in two-dimensional and axially-symmetric nozzles. Quart. J. Mech. App. Maths., 15, part 4, pp. 487–508, November 1962.
2	W. T. Lord	A theoretical study of annular supersonic nozzles. A.R.C., R & M 3227, 1961.
3	G. M. Edelman	The design, development and testing of two-dimensional sharp-cornered supersonic nozzles. Meteor Report No. 22 (M.I.T.), May 1948. Gas Turbine Laboratory, Guided Missiles Programe.
4	H. Shames and F. L. Seashore	Design data for graphical construction of two-dimensional sharp-edge-throat supersonic nozzles. NACA RM No. E8J12. TIB./1903.
5	A. Busemann	Handbuch der Experimental-physik, 4, p. 407, 1931.
6	A. E. Puckett	Supersonic nozzle design. J. App. Mechanics, 13, No. 4, pp. A265–A270, December 1946.
7	A. O. L. Atkin	Two-dimensional supersonic channel design. Part I. A.R.C., R & M 2174, 1945.
8	K. Foelsch	A new method of designing two-dimensional Laval nozzles for a parallel and uniform jet. N.A.A. Report NA–46–235, 1946.
9	I. E. Beckwith and J. A. Moore	An accurate and rapid method for the design of supersonic nozzles. N.A.C.A. TN 3322, 1955.
10	K. O. Friedrichs	Theoretical studies on the flow through nozzles and related problems. App. Maths Panel 82–IR, AMG–NYU No. 43, New York University, April 1944.
11	E. Nilson	Analytic correction of a two-dimensional nozzle for uniform exhaust flow. U.A.C. Meteor Report No. 15, 1948.

REFERENCES—*continued*

No.	*Author(s)*	*Title, etc.*
12	J. R. Baron	Analytic design of a family of supersonic nozzles by the Friedrichs method. W.A.D.C. Technical Report 54–279, June 1954.
13	H. N. Riise	Flexible-plate nozzle design for two-dimensional supersonic wind tunnels. J.P.L. Report No. 20–74, C.I.T., June 1954.
14	J. Rosen	The design and calibration of a variable Mach number nozzle. J. Aeronaut. Sci., 22, No. 7, pp. 484–490, 1955.
15	J. C. Sivells	Design of two-dimensional continuous-curvature supersonic nozzles. J. Aeronaut. Sci., 22, No. 10, pp. 685, 692, 1955.
16	H. Görtler	Zum Übergang von Unterschall-zu Überschallgeschwindigkeiten in Düsen. Zett angew Math Mech, 19. No. 6, pp. 325, 337, 1939.
17	D. Bershader	An interferometric study of supersonic channel flow. Rev. of Sci. Inst., 20, No. 4, 1949.
18	E. W. E. Rogers and Miss B. M. Davis ..	A note on turbulent boundary layer allowances in supersonic nozzle design. A.R.C. C.P. 333, 1957.
19	M. Sibulkin	Heat transfer to an incompressible turbulent boundary layer and estimation of heat-transfer coefficients at supersonic nozzle throats. J. Aeronaut. Sci., 23, No. 2, pp. 162–172, 1956.
20	S. Neumark	Solution of cubic and quartic equations. R.A.E. TN Aero 2843, October 1962.
21	G. Temple	The method of characteristics in supersonic flow A.R.C. R & M 2091, January 1944.
22	M. G. Hall	The accuracy of the method of characteristics for plane supersonic flow. Quart. J. Mech. App. Maths., 9, pt. 3., pp. 320, 333, 1956.
23	H. N. Riise	Functions of Prandtl-Meyer angle for supersonic nozzle design. J.P.L. Publication No. 26, C.I.T., December 1953.
24	D. E. Hartley	A.R.C. 16,780, 1953.
25	J. Ruptash	Supersonic wind tunnels-theory, design and performance. UTIA Review No. 5, 1952.

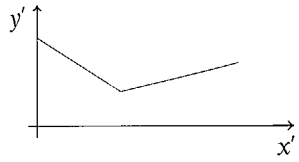

TABLE I

Boundary-Layer Corrected Nozzle Co-ordinates

All Dimensions in Inches

x'	y'
0·0000	2·6360
0·5000	2·4097
1·0000	2·1848
1·5000	1·9618
2·0000	1·7414
2·5000	1·5248
3·0000	1·3138
3·5000	1·1117
4·0000	0·9241
4·5000	0·7616
4·6000	0·7336
4·7000	0·7075
4·8000	0·6835
4·9000	0·6619
5·0000	0·6428
5·1000	0·6265
5·2000	0·6131
3·3000	0·6029
5·4000	0·5960

x'	y'
5·5000	0·5924
5·5957	0·5962
5·6823	0·6033
5·7812	0·6122
5·9096	0·6289
6·0159	0·6478
6·1438	0·6747
6·2892	0·7085
6·4291	0·7434
6·5755	0·7836
6·6636	0·8082
6·8324	0·8574
6·9493	0·8924
7·0804	0·9330
7·3283	1·0104
7·5008	1·0645
7·5807	1·0897
7·7265	1·1357
7·8414	1·1719

x'	y'
8·0561	1·2395
8·3488	1·3294
8·5615	1·3928
8·9019	1·4897
9·2759	1·5893
9·6865	1·6911
10·1373	1·7946
10·6322	1·8992
11·1753	2·0042
11·7716	2·1088
12·4262	2·2119
13·1447	2·3123
13·9339	2·4086
14·8006	2·4992
15·7529	2·5819
16·7996	2·6545
17·9504	2·7142
19·2166	2·7577
20·0316	2·7759

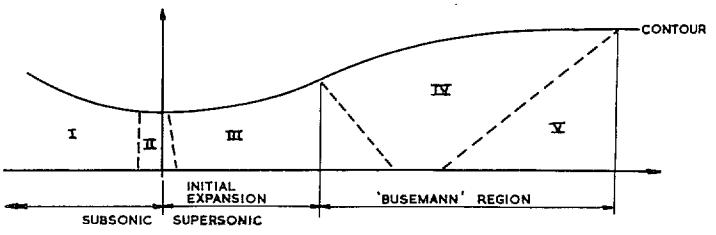

FIG. 1. The principal regions of a supersonic nozzle.

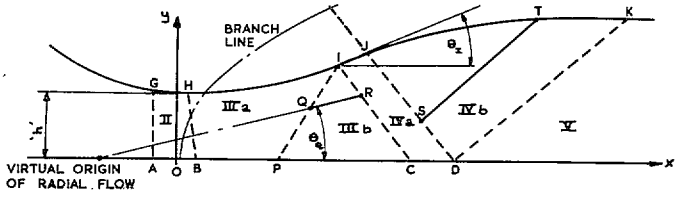

FIG. 2. The particular regions relevant to the nozzle design.

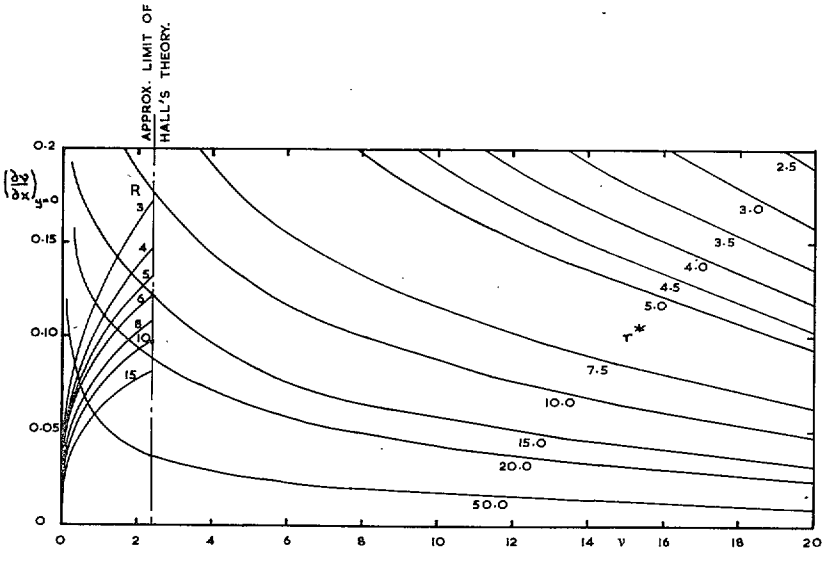

FIG. 3. $\left(\frac{\partial v}{\partial x}\right)_{y=0}$ in the throat and in the radial flow plotted against ν.

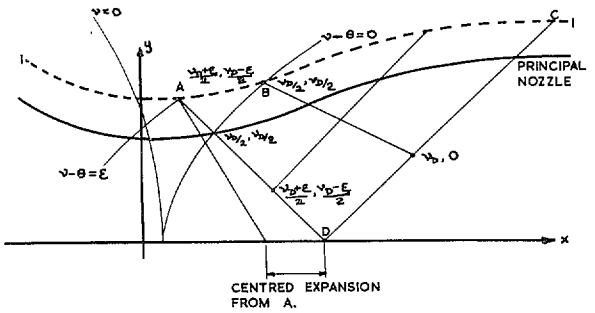

FIG. 4. Sketch of streamlines and characteristics relevant to discussion on minimum-length nozzle.

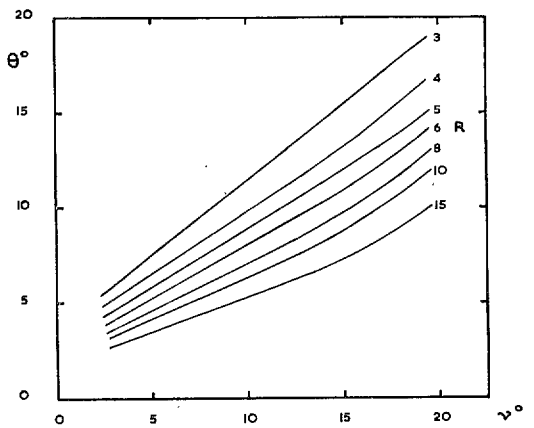

FIG. 5. Curves of θ against ν to aid the selection of R, ν_p and θ_r.

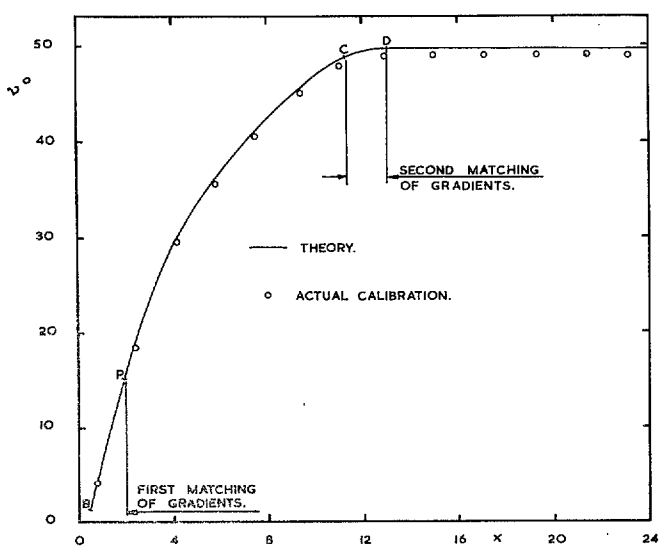

FIG. 6. Variation of Prandtl-Meyer angle along nozzle axis.

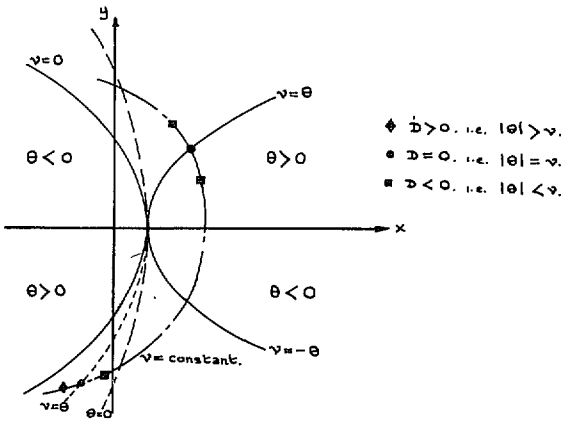

FIG. 7. Sketch illustrating locations of roots of equation (B.9). $P>0$.

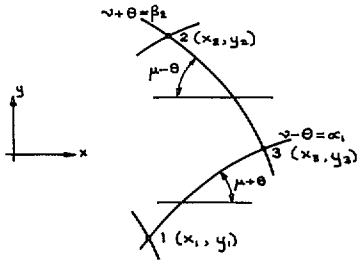

FIG. 8. Sketch of a typical characteristic mesh.

Printed in Wales for Her Majesty's Stationery Office by Allens (Cardiff) Limited

Dd.125874 K 5

Published by
HER MAJESTY'S STATIONERY OFFICE

To be purchased from
49 High Holborn, London w.c.1
423 Oxford Street, London w.1
13A Castle Street, Edinburgh 2
109 St. Mary Street, Cardiff
Brazennose Street, Manchester 2
50 Fairfax Street, Bristol 1
35 Smallbrook, Ringway, Birmingham 5
7–11 Linenhall Street, Belfast 2
or through any bookseller

S.O. Code No. 23–3440